13th World Conference on Earthquake Engineering
Vancouver, B.C., Canada
August 1-6, 2004
Paper No. 374

MECHANICS AND DESIGN OF BARE TYPE SRC COLUMN BASES UNDER SEVERE SEISMIC LOAD

Kazushi SADASUE[1] and Koichi MINAMI[2]

SUMMARY

A large number of Steel Reinforced Concrete (SRC) buildings were damaged owing to 1995 Hyogoken-Nanbu earthquake in Japan. We focused on the failure of column bases in these damages. The design method of column bases can be divided roughly into bare type and embedded type column bases. Bare type column bases were damaged on Hyogoken-Nanbu earthquake, in comparison with embedded type column bases. It is thought that the tension forced due to overturning moment is the reason why these damages. Therefore, it might be dangerous to use bare type column bases for the SRC structures under severe seismic load. However, since the design method of using bare type column bases is advantageous for the workability and the economy, we would like to use bare type column bases for SRC buildings.

In the beginning, we confirmed the mechanical behavior of bare type column bases through structural tests under a high tensile axial load and a cyclic horizontal load. The structural tests make it clear that ultimate flexural strength under a tensile axial force can be evaluated by AIJ standard, but, in the AIJ standard, the evaluation method of deformation capacity remains unanswered. In order to design SRC buildings under severe earthquake, it is essential to evaluate the ductility. Therefore, we tried to evaluate elasto-plastic behavior of column bases by using the kinematical model. To use the kinematical model, we proposed the equilibrium condition, compatibility condition and constitutive equation in column bases, and the hysteresis characteristics was calculated according to the fiber model.

From the structural tests and the elasto-plastic analysis, seismic performance of bare type column bases under a high tensile axial force were became clear, and we showed the problem which we have to consider for structural design of bare type column bases under a high variable axial force.

INTRODUCTION

It was reported that Steel Reinforced Concrete (SRC) buildings were damaged seriously owing to 1995 Hyogoken-Nanbu earthquake in Japan [1]. We focused on the failure of column bases in these damages. The design method of SRC column bases can be divided roughly into bare type and embedded type bases. Bare type column bases doesn't bury the column steel in the reinforced concrete (RC) footing beam, and

[1] Center for High-Tech Research, Fukuyama University, Fukuyama, Japan. Email: k_sadasue@hotmail.com
[2] Dept. of Architecture, Faculty of Eng., Fukuyama University, Fukuyama, Japan. Email: minami@fucc.fukuyama-u.ac.jp

the column steel is set on the surface of footing beam, and connected with the footing beam by anchor bolts. Bare type column bases had been multiuse before Hyogoken-Nanbu earthquake on the grounds that it is advantageous for the workability and the economy. However, bare type column bases were damaged on Hyogoken-Nanbu earthquake, in comparison with embedded type column bases. According to the report, it is thought that the tension forced due to overturning moment is the reason why the damage of column bases. Good earthquake resistant design in the SRC buildings requires a deep knowledge of how column bases behave under a high tensile axial loading.

This paper presents the result of the structural tests carried out in order to study elasto-plastic behavior of bare type column bases in SRC structure. In addition, the analytical method of the hysteresis characteristics of SRC columns using bare type column bases was shown. The main discussion is concentrated on the maximum strength, the ductility after the attainment of the maximum strength.

EXPERIMENTAL WORK

Specimen descriptions

The specimen is a cantilever that assumes the behavior below an inflection point of the column of first floor in SRC buildings. A total of 15 specimens were tested to investigate the elasto-plastic flexural behavior of bare type column bases. Table 1 shows test program, and the bar arrangements and dimensions are shown in fig. 1 and in fig. 2, respectively. The specimens had a column section of 400mm×400mm, and a column steel was using H-250×125×6×9 (Grade SM490). Moreover, all specimens were designed so that the failing in a flexural mode happened earlier than the failing in a shear mode. The following experimental parameters were selected: a tensile axial load level and the composition of column bases section. The mechanical properties of concrete cylinder and steel are shown in Table 2 and in Table 3, respectively.

Table 1 Test program

Specimen	Column Section	Axial load	Maximum Axial load N (kN)		Reinforcement	Anchor bolt	Material Strength Classification
			Compression	Tension			
C0A	Type A	Constant load	-	0 (n_t=0)	16-D13(SD345)	4-M24(SS490)	Series I
C0B	Type B				20-D13(SD345)	4-M18(SS490)	
C0C	Type C				24-D13(SD345)	4-M12(SS400)	
C4A	Type A		-	-500 (n_t=-0.40)	16-D13(SD345)	4-M24(SS490)	
C4B	Type B				20-D13(SD345)	4-M18(SS490)	
C4C	Type C				24-D13(SD345)	4-M12(SS400)	
C8A	Type A		-	-1000 (n_t=-0.80)	16-D13(SD345)	4-M24(SS490)	Series II
C8B	Type B				20-D13(SD345)	4-M18(SS490)	
C8C	Type C				24-D13(SD345)	4-M12(SS400)	
V4A	Type A	Fluctuating load	1650 (n_c=0.26)	-500 (n_t=-0.40)	16-D13(SD345)	4-M24(SS490)	Series III
V4B	Type B				20-D13(SD345)	4-M18(SS490)	
V4C	Type C				24-D13(SD345)	4-M12(SS400)	
V8A	Type A		2960 (n_c=0.46)	-1000 (n_t=-0.80)	16-D13(SD345)	4-M24(SS490)	
V8B	Type B				20-D13(SD345)	4-M18(SS490)	
V8C	Type C				24-D13(SD345)	4-M12(SS400)	

Axial compression : positive, Axial tension : negative

$n_c = N / N_{cu}$

$n_t = N / N_{tu}$

$N_{cu} = B \cdot D \cdot \sigma_c$

$N_{tu} = {}_a n \cdot {}_a A \cdot {}_a\sigma_y + {}_m n \cdot {}_m A \cdot {}_m\sigma_y$

B, D, σ_c: Column width, Column depth, Compressive strength of concrete

${}_a n$, ${}_a A$, ${}_a\sigma_y$: Number of anchor bolt, Sectional area of anchor bolt, Yield stress of anchor bolt

${}_m n$, ${}_m A$, ${}_m\sigma_y$: Number of main reinforcement, Sectional area of main reinforcement, Yield stress of main reinforcement

All specimens have been tested using the test setup system as shown in fig.3. The footing beam was fixed to the loading bed. Between the loading frame and the top of the specimen, there was the rotational pin to ensure the corresponding relative displacement of the top and the bottom of column. Axial load N and lateral load H was applied by the oil jacks connected to the loading frame. All specimens were subjected to a cyclic lateral load and a tensile axial load (constant or fluctuating axial load). The constant tensile axial load level was at three stages (n_t=-0, -0.40 and -0.80). The fluctuating tensile axial load level was at two stages (n_t=-0.40~n_c=0.26 and n_t=-0.80~n_c=0.46). The cyclic lateral loading is applied on every deflection angle R=0.005rad. under displacement control, where R means the value in which lateral displacement δ_{UC} of top of the column is divided by shear span L.

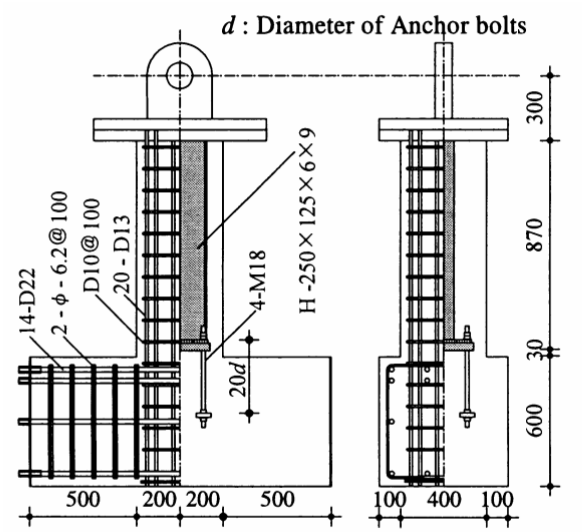

Fig. 1 Test specimen V4B (Unit : mm)

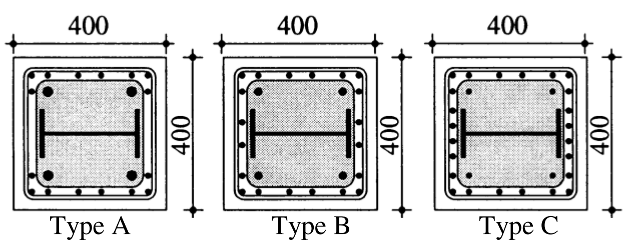

Fig. 2 Section of column (Unit : mm)

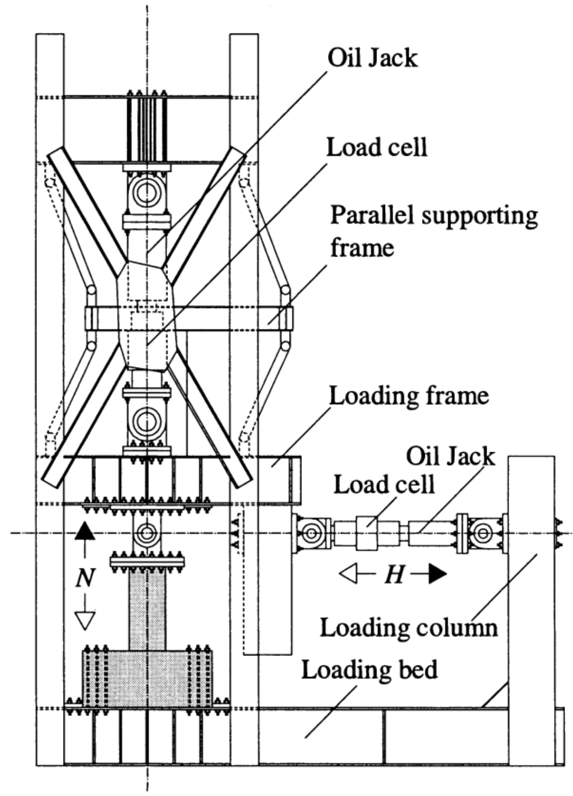

Fig. 3 Test setup system

Table 2 Mechanical properties of concrete

Series	Concrete	Compressive strength σ_c (N/mm^2)	Cleavage strength σ_t (N/mm^2)	Young's modulus E (N/mm^2)
Ⅰ	Column	24.2	2.19	2.50×10^4
	Footing beam	26.2	2.20	2.08×10^4
	Grout mortal	30.2	2.91	-
Ⅱ	Column	32.1	2.57	2.75×10^4
	Footing beam	50.0	3.46	3.19×10^4
	Grout mortal	56.1	4.18	2.52×10^4
Ⅲ	Column	40.0	2.51	3.12×10^4
	Footing beam	67.0	2.80	3.62×10^4
	Grout mortal	58.1	3.68	2.43×10^4

Table 3 Mechanical properties of steel

Series	Steel		Yield stress σ_y (N/mm^2)	Tensile stress σ_u (N/mm^2)	Elongation (%)	Young's modulus E (N/mm^2)
I	Steel bar	D13	371	536	22.2	1.94×10^5
		D10	384	521	20.0	1.69×10^5
	Anchor bolt	M24	339	525	27.0	1.85×10^5
		M18	343	542	22.8	2.12×10^5
		M12	328	462	29.3	1.67×10^5
	Steel flange	PL9	325	433	26.0	1.96×10^5
	Steel web	PL6	374	448	23.0	1.90×10^5
II	Steel bar	D13	373	564	18.9	1.67×10^5
		D10	350	492	23.4	1.81×10^5
	Anchor bolt	M24	345	541	27.3	1.95×10^5
		M18	337	538	24.1	2.01×10^5
		M12	310	474	31.3	2.05×10^5
	Steel flange	PL9	305	446	25.2	2.03×10^5
	Steel web	PL6	462	557	12.0	1.98×10^5
III	Steel bar	D13	391	564	17.6	1.77×10^5
		D10	449	504	17.7	1.90×10^5
	Anchor bolt	M24	331	523	25.3	1.77×10^5
		M18	358	555	23.0	1.72×10^5
		M12	327	457	30.1	1.92×10^5
	Steel flange	PL9	393	546	17.2	1.61×10^5
	Steel web	PL6	402	553	16.7	1.68×10^5

Hysteresis characteristics

Relationships of lateral load H and deflection angle R are shown in Fig.4. In these figures slight solid lines indicate the ultimate flexural strength Q_{fu} which is obtained by AIJ standard [2].

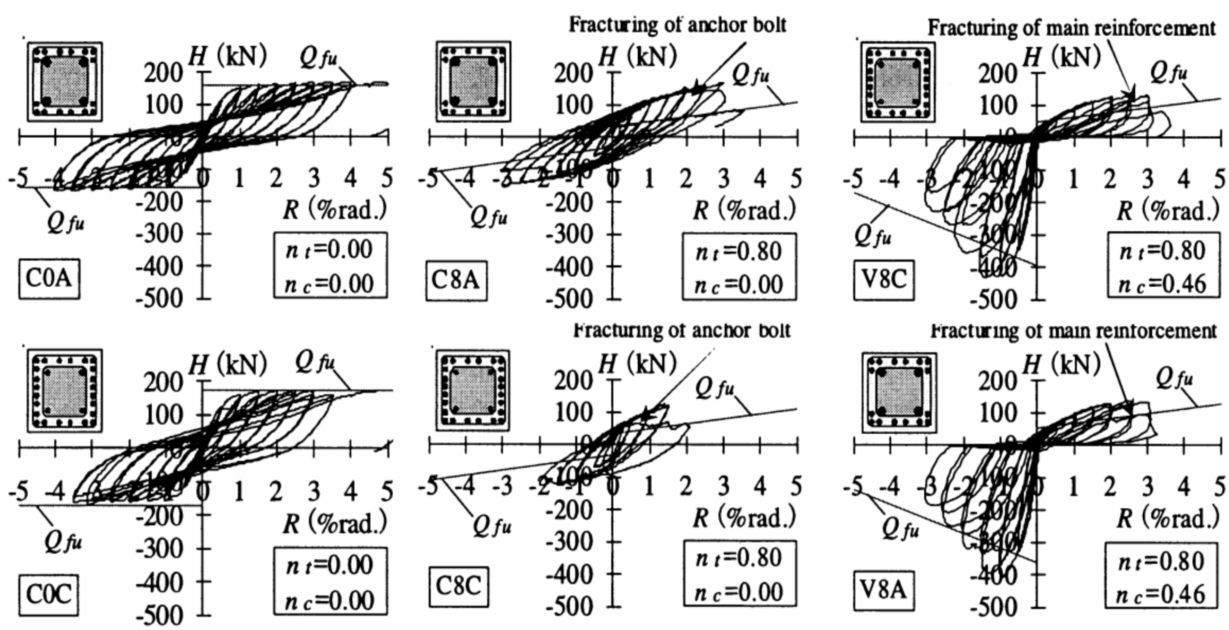

Fig. 4 Relationships of lateral load and deflection angle

It is observed in the relationships on the constant tensile axial load level n_t=0 that the hysteresis loop have some pinching. However, the degradation of strength due to repetition of the loading is small, and the ductility is large. The hysteresis loop on the constant tensile axial load level n_t=0.8 are spindle shaped, but strength then decreases rapidly by fracturing the anchor bolt on R=1.5~3.0%rad.. When the specimens doesn't have the tensile axial force, one of the reasons why the hysteresis loop shows the slipping properties is that anchor bolts are causing of the plastic elongation. In the loading after the anchor bolts are causing of the plastic elongation, a tensile force doesn't act on the anchor bolts just behind the unloading. The characteristic of pinching doesn't appear easily in the hysteresis loop because anchor bolts and base plate always engage under the high constant tensile axial force. In the other hand, the influence of the buckling of main reinforcement appeared remarkably in the hysteresis characteristics under the fluctuating axial force. The buckling of main reinforcement and the fracturing after the buckling of main reinforcement caused a rapid strength decrease.

Ultimate strength

Relationships of axial force N and ultimate bending moment M_u by AIJ standard are shown in fig. 5. The compressive axial force is assumed to be positive. Dotted points mean the experimental values. Fig. 6 shows the relationships of the experimental value ${}_{exp}M_u$ and the calculation value ${}_{cal}M_u$ of all specimens. The calculation values by AIJ standard is calculated to the method of the superposed strength. It is seen from fig. 5 and fig. 6 that the calculation values evaluate ultimate strength to safety side. The experimental values under a high tensile axial force are thought to be largely due to the influence of the strain hardening.

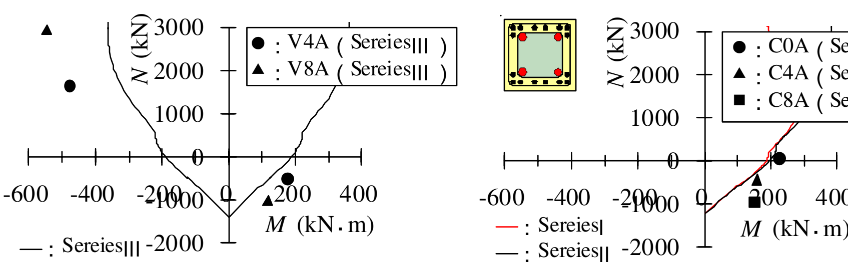

Fig. 5 Relationships of axial force and ultimate bending moment

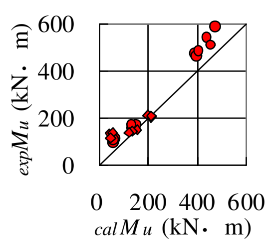

Fig. 6 Calculation accuracy

Limit deflection angle

Fig. 7 shows the limit deflection angle of SRC columns using bare type column base. The limit deflection angle under a tensile axial force R_{tu} means the deflection angle when main reinforcement or anchor bolts fractured. The limit deflection angle under the compressive axial force R_{cu} means the deflection angle when the strength decreased from the maximum strength by 20%. However, the specimens which don't reach R_{tu} and/or R_{cu} show the maximum deflection angle in the experiment. Equation (1) was proposed as an evaluation equation of the limit deflection angle [3]. This equation is the empirical equation induced from the experimental study carried out after Hyogoken-Nanbu earthquake.

$$R_{tu} = 0.088 - 0.07\, n_t \qquad (1)$$

The experimental values have unsafe-side error of Equation (1). Especially, the ductility is small under the varying axial force. Fracturing is caused easily under the fluctuating axial force so that the main reinforcement may repeat the buckling and the plasticity elongation.

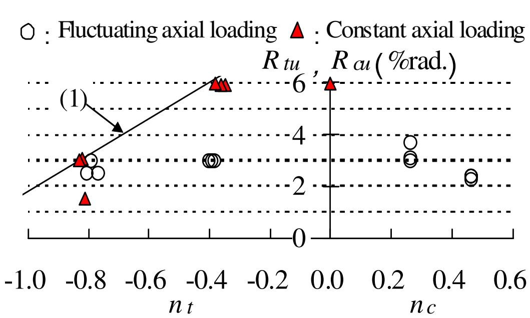

Fig. 7 Limit deflection angle

ANALYSIS METHOD

Analytical model

The proposed analytical model objects bare type column bases failing in a flexural mode (photo 1).

V8A

Photo 1 Final destruction state

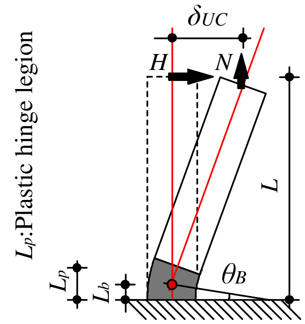

Fig. 8 Analytical model

The deflection angle of SRC columns using bare type column base under an axial force N and a lateral force H are assumed the model shown in Fig. 8, and the bending moment of column base M_B and the deflection angle R is given as:

$$M_B = H \times (L - L_b) + (N \times \delta_{UC}) \tag{2}$$
$$R = \delta_{UC} / L \tag{3}$$
$$\delta_{UC} = \theta_B \, (L - L_b) \tag{4}$$

Where, L means shear span, and L_b means position of the base plate.

Compatibility condition and equilibrium condition

Relationships of M_B and θ_B can be calculated according to the fiber model in fig. 9 and fig. 10. Here, concrete was divided into the layer elements into 60, and main reinforcement and anchor bolts were one element, respectively.

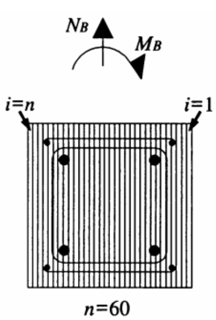

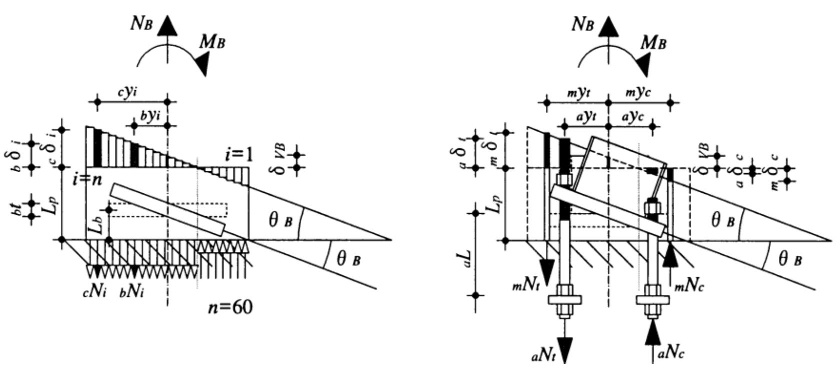

(a) Elements of concrete (b) Elements of main reinforcement and anchor bolt

Fig. 9 Division of section

Fig. 10 Compatibility condition and equilibrium condition

Displacement and strain of each element follows compatibility condition in fig. 10. It is assumed that the column steel and the base plate to be a rigid body. Compatibility condition is expressed as the follow:

$$_c\delta_i = \theta_B \times {_cy_i} + \delta_{VB} \tag{5}$$
$$_b\delta_i = \theta_B \times {_by_i} + \delta_{VB} \tag{6}$$
$$_m\delta_t = \theta_B \times {_my_t} + \delta_{VB} \tag{7}$$
$$_m\delta_c = \theta_B \times {_my_c} + \delta_{VB} \tag{8}$$
$$_a\delta_t = \theta_B \times {_ay_t} + \delta_{VB} \quad ({_a\delta_t}<0) \tag{9}$$
$$_a\delta_c = \theta_B \times {_ay_c} + \delta_{VB} \quad ({_a\delta_c}<0) \tag{10}$$

$_c\varepsilon_i = {}_c\delta_i \,/\, L_p$ (11) $\quad$ $_b\varepsilon_i = {}_b\delta_i \,/\, (L_p - {}_bt)$ (12)

$_m\varepsilon_t = {}_m\delta_t \,/\, L_p$ (13) $\quad$ $_m\varepsilon_c = {}_m\delta_c \,/\, L_p$ (14)

$_a\varepsilon_t = {}_a\delta_t \,/\, {}_aL \quad ({}_a\delta_t<0)$ (15) $\quad$ $_a\varepsilon_c = {}_a\delta_c \,/\, {}_aL \quad ({}_a\delta_c<0)$ (16)

where,

$_c\delta_i$, $_b\delta_i$, $_m\delta_t$, $_m\delta_c$, $_a\delta_t$, $_a\delta_c$:displacement of concrete surrounding the base plate, concrete upper and lower the base plate, main reinforcement on tension side, main reinforcement on compression side, anchor bolt on tension side, anchor bolt on compression side, respectively.

$_c\varepsilon_i$, $_b\varepsilon_i$, $_m\varepsilon_t$, $_m\varepsilon_c$, $_a\varepsilon_t$, $_a\varepsilon_c$:strain of concrete surrounding the base plate, concrete upper and lower the base plate, main reinforcement on tension side, main reinforcement on compression side, anchor bolt on tension side, anchor bolt on compression side, respectively.

L_p, $_aL$:plastic hinge length and anchorage length of anchor bolt, respectively.

$_bt$:thickness of the base plate.

M_B and N_B can be calculated as follows:

$$N_B = N = {}_cN_i + {}_bN_i + {}_mN_t + {}_mN_c + {}_aN_t + {}_aN_c \tag{17}$$

$$M_B = {}_cN_i \times {}_cy_i + {}_bN_i \times {}_by_i + {}_mN_t \times {}_my_t + {}_mN_c \times {}_my_c + {}_aN_t \times {}_ay_t + {}_aN_c \times {}_ay_c \tag{18}$$

Plastic hinge length

When the strain of main reinforcement and concrete is calculated, it is necessary to decide the plastic hinge length L_p beforehand. L_p uses a different value in the plastic hinge length on bend compression side L_{pc} [4] and the plastic hinge length on bend tension side L_{pt} [5]. L_{pc} and L_{pt} are calculated by the following equations, respectively.

$$L_{pc} = (0.1 + 1.3 \times D \,/\, L) \times L \tag{19}$$

$$L_{pt} = \{(435 - {}_cL) \,/\, 768 \times n^2 + {}_cL \,/\, 1200\} \times L \tag{20}$$

Where, $_cL$ means distance from the joint surface of column-beam to the cone crack caused from edge of the base plate, and n means the tensile axial force ratio on bend tension side.

Constitutive equation

Stress-strain relations used in the analysis are shown in Fig.11. Notation σ designates the stress. Stress-strain curves of concrete were considered confinement effect of the lateral reinforcement [6]. Naganuma's proposed model [7] was adopted in unloading. The skeleton curve of main reinforcement was assumed to be trilinear model. Cyclic stress-strain curve was considered Bauschinger effect [7]. The skeleton curve of anchor bolt was assumed to be Yoshizumi's proposed model [8]. It is assumed that the anchor bolts resist tensile force only.

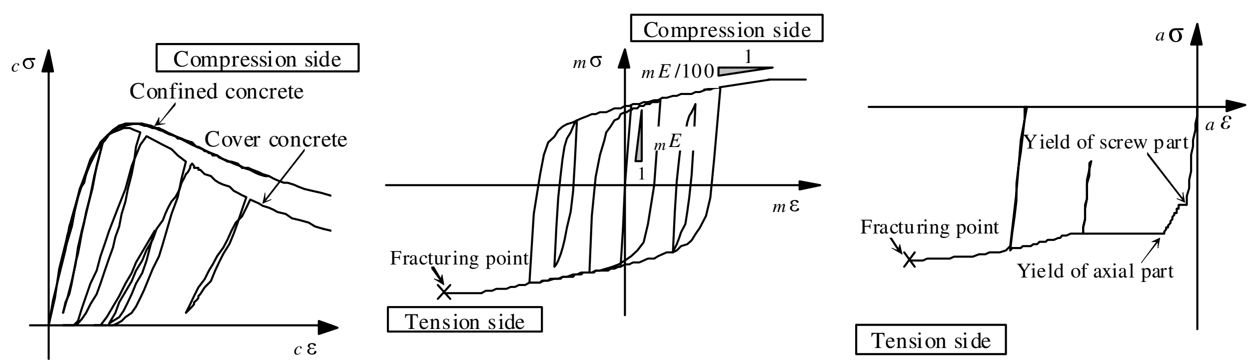

(a) Concrete (b) Main reinforcement (c) Anchor bolt

Fig. 11 Stress-strain relations

Analytical results

Fig.12 shows the relationships of M_B and R. The analytical values indicate only the maximum value of deflection angle in each hysteresis loop. The analytical values well predicts the experimental results. However, it is necessary to careful attention that the proposed analytical method doesn't consider the buckling and fracturing after buckling of main reinforcement. Therefore, the compressive axial force ratio should still be kept below a limiting value to use the proposed analytical method.

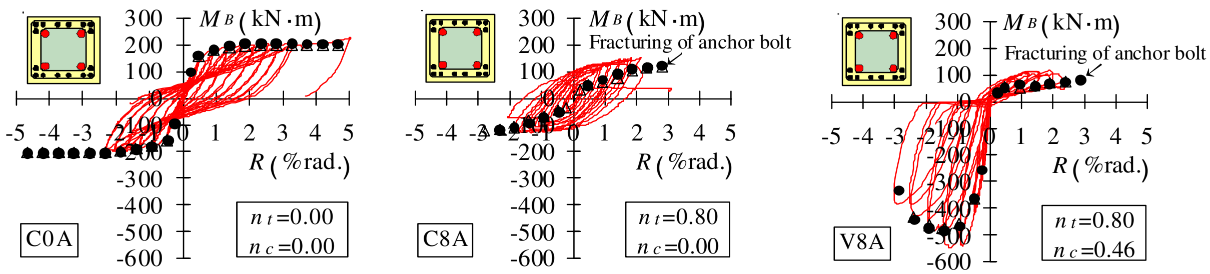

Fig. 12 Relationships of bending moment and deflection angle

CONCLUSIONS

Through the experiments conducted in this study, structural performance of bare type column bases under a high tensile axial force were became clear, and we showed that the mechanical property can be evaluated by the proposed analysis method. SRC columns used bare type column base shown by this paper are necessary to keep in mind that strength of the column section with steel is strong enough compared with strength of the column base section. However, if strength of the column section is small compared with strength of the column base section, it doesn't seem that the seismic performance becomes disadvantageous to approach the properties of usual SRC columns.

REFERENCES

1. AIJ: Editorial Committee for the Report on the Hanshin-Awaji Earthquake Disaster, Report on the Hanshin-Awaji Earthquake Disaster, Building Series Volume 2, Structural Damage to Steel Reinforced Concrete Buildings, 1998
2. AIJ: Standard for Structural Calculation of Steel Reinforced Concrete Structures, 2001
3. Ryoichi S, Yoshikazu S, Kazumasa I, Haruo N, Hiroyuki N, Toshiyuki F: Strength and Ductility of Unembedded Type of Steel Reinforced Concrete Column Base under Tensile Force, J. Struct. Constr. Eng., AIJ, No.569, 2003: 111-118
4. Junichi S, Chiaki M: Hysteresis Characteristic of Steel Reinforced Concrete Beam-Columns, J. Struct. Constr. Eng., AIJ, No.534, 2000: 183-190
5. Kazushi S, Daiei F, Michio I, Hideniri T, Koichi M: Analytical Study on Structural Behavior of Bare Type Column Base Connection in SRC Structures under Varying Axial Force, Proceedings AIJ Tyugoku Chapter Architectural Research meeting, AIJ Tyugoku Chapter, No.26, 2004
6. Kenji S, Yuping S: An Analytical Model for Reinforced Concrete Panels under Cyclic Stresses, J. Struct. Constr. Eng., AIJ, No.536, 2000: 135-142
7. Kazuhiro N, Masaaki O: Stress-Strain Curve of Concrete Confined by Rectilinear Hoop, J. Struct. Constr. Eng., AIJ, No.461, 1994: 95-104
8. Isao H, Takasi Y, Noriyoshi D, Chiaki M: Tension Characteristics of Anchor bolt with cut threads at both ends (part 1,2,3), summaries of technical papers presented at annul meeting of AIJ, 1999: 661-666